The Electrochemical Behavior of Ti-6Al-7Nb Alloy with and without Plasma-Sprayed Hydroxyapatite Coating in Hank's Solution

I. C. Lavos-Valereto,[1] I. Costa,[2] S. Wolynec[1]

[1] Department of Metallurgical and Materials Engineering, Polytechnic School of the University of São Paulo, Av. Prof. Mello Moraes, 2463–CEP 05508-900, São Paulo, SP, Brazil

[2] Materials Science and Technology Centre, IPEN/CNEN, São Paulo, SP, Brazil

Received 5 October 2001; revised 11 March 2002; accepted 21 March 2002
Published online 22 August 2002 in Wiley InterScience (www.interscience.wiley.com). DOI: 10.1002/jbm.10351

Abstract: The electrochemical behavior of Ti-6Al-7Nb alloy with and without plasma-sprayed hydroxyapatite (HA) coating was investigated in Hank's balanced salt solution at 37 °C. This behavior was evaluated by analyzing both corrosion potential variation with time curves and potentiodynamic polarization curves. The polarization curves were determined both in aerated and deaerated solutions. It was found that the corrosion potential of uncoated sample is always more noble than that of coated one. In aerated solutions the polarization curve of a coating-free alloy presents a typical passive/transpassive behavior, which is absent in the HA-coated alloy and in deaerated solution for both coated and uncoated conditions. In the latter polarization curves, the current density continuously increases with the increase of the potential. The corrosion rate determined from polarization curves is higher for HA-coated alloys, but it still can be considered negligible (less than 1 $\mu A/cm^2$). © 2002 Wiley Periodicals, Inc. J Biomed Mater Res (Appl Biomater) 63: 664–670, 2002

Keywords: titanium alloy; hydroxyapatite; corrosion; biomaterial; dental implant

INTRODUCTION

In order to fulfill their function, metallic implants must, first be accepted by the body. This acceptance, or biocompatibility, is improved when the surface in contact with living tissues is coated with a ceramic material capable of forming a strong chemical bond with natural bone. Calcium-phosphate-bearing ceramics, especially hydroxyapatite (HA), are the most suitable coatings for this purpose.[1,2] Hydroxyapatite is the inorganic component of bones and teeth. It has been identified as a bioceramic with bioactive properties suitable for bone substitution and interfacing layers in surgical implants. Hydroxyapatite [$Ca_{10}(PO_4)_6(OH)_2$] has a similar mineral constitution to that of bone, and its high calcium and phosphorous components favor tissue response by accelerating and enhancing fixation to hard bone without the interaction of soft tissue.[3] It can, also enhance early bone tissue formation in porous coatings such that full weight bearing can be allowed much sooner after surgery.[4]

Some implants are made of titanium or a titanium alloy coated with a thin layer of hydroxyapatite, applied by the plasma spray technique. It is believed that this coating can reduce the metal-ion release-kinetics, simply by acting as a physical barrier. On the other hand, this coating must be porous in order to assure good osseointegration.[5–7] However, the coating porosity may affect the corrosion behavior of metal implants. The corrosion of biomaterials is critical and can adversely affect biocompatibility and/or mechanical integrity.[8–10]

Currently, titanium or titanium-aluminum-vanadium alloys are the metallic materials of choice for endosseous implants. More recently, the Ti-6Al-7Nb alloy has been also considered for this application. In two previous works the histological responses,[3] and in vitro and in vivo biocompatibility[11] of the latter alloy with and without plasma-sprayed hydroxyapatite were investigated. *In vivo* tests carried out in mongrel dogs showed a satisfactory osseointegration in both coated and uncoated alloys.

The aim of the present work was to evaluate the effect of hydroxyapatite coating on the electrochemical behavior of Ti-6Al-7Nb alloy in Hank's solution, which simulates the body environment. This behavior was evaluated by analyzing both corrosion potential variation with time curves and potentiodynamic polarization curves, obtained for both coated

Correspondence to: I. C. Lavos-Valereto, Department of Metallurgical and Materials Engineering, Polytechnic School of the University of São Paulo, Av. Prof. Mello Moraes, 2463–CEP 05508-900, São Paulo, SP, Brazil (e-mail: ielvaler@usp.br)

Contract grant sponsor: Fundação de Amparo à Pesquisa do Estado de São Paulo—FAPESP (São Paulo State Foundation for Support of Research); contract grant numbers: FAPESP 99/08554-6 and FAPESP 99/03771-9

TABLE I. Semiquantitative Chemical Composition of Ti-6Al-7Nb Alloy Determined by EDS Analysis

	Element		
	Ti	Al	Nb
wt%	89.78	4.64	5.58

and uncoated titanium alloy samples. The obtained data can be valuable for estimation of implant corrosion resistance and for anticipation of their effect upon possible biochemical and cellular events at the bone–implant interface.

EXPERIMENT

The semiquantitative chemical compositions of the Ti-6Al-7Nb alloy and the hydroxyapatite coating deposited by plasma spraying are given in Tables I and II, respectively. These compositions were determined by energy-dispersive spectroscopy (EDS) analysis.

The samples used in this investigation consisted of small cylindrical-shaped screws 10 mm long and with a diameter of about 4.0 mm. The shape of these samples is shown in Figure 1. The coating procedure (hydroxyapatite by plasma spraying) is described elsewhere.[6] Figure 2 is a scanning electron micrograph (SEM) of the hydroxyapatite-coated screw surface. Note that the metallic surface is totally covered and that the coating is porous.

The electrochemical tests were run in a single dark glass electrochemical cell containing 600 ml of Hank's balanced salt solution (HBSS), the composition of which is given in Table III. Instituto Adolpho Lutz, São Paulo, Brazil, prepared this solution. A saturated calomel electrode (SCE) was used as the reference electrode, and a graphite rod was used as the counter electrode. Both aerated and deaerated tests were carried out in a thermostatic bath at (37.0 ± 0.1) °C. In deaerated tests the sample was already inside the solution during the deaeration process. Nitrogen was purged for at least 2 h before the beginning of these tests, and purging was continued during the tests. Prior to immersion in Hank's solution the upper part of the specimens was protected with epoxy resin (epo-kwick resin, Buehler, Chicago, IL), as shown in Figure 1.

Both the corrosion potential measurements and the potentiodynamic polarization curves were obtained with a Princeton Applied Research potentiostat (Model 273A). A microcomputer was used for the data acquisition. The potentiodynamic measurements were started after a 2-h immersion in the physiological solution. The scanned potential range varied from −800 mV below the corrosion potential up to 3000 mV (SCE). The scanning rate was 1 mV/s. The corrosion potential measurements were performed over 0–8 h.

RESULTS

Figure 3 shows the corrosion potential E_{corr} variation with time for a 0–8-h period, for both specimens, coated and uncoated, in Hank's solution at 37 °C. This figure shows that for the uncoated sample the initial corrosion potential is around −210 mV (SCE), and then it gradually increases over about 1.5 h until an approximately steady value is reached. For the coated sample the initial corrosion potential is about −230 mV (SCE), and during the first 30 min its value tends to decrease; then it starts to increase until a steady value is reached after about 2 h. It can be noticed that the steady potential of the uncoated specimen is more noble [approximately −100 mV (SCE)] than that of coated specimen [nearly −140 mV (SCE)]. The potential of the coated specimen also shows a large number of oscillations, mainly in the beginning of the test, while that of the uncoated alloy shows only two oscillations.

The recording of E_{corr} was interrupted after 8 h, but the sample remained immersed inside the testing solution for 24 h. At this time the measured E_{corr} values were −60 mV (SCE) and −170 mV (SCE) for the uncoated and coated specimens, respectively, which indicates that there is not a real stabilization of E_{corr} during this period of time, because it continued to increase slowly.

In order to obtain reliable results, the determination of potentiodynamic polarization curves was repeated nine times in aerated Hank's solution and three times in deaerated solution.

The typical potentiodynamic polarization curves of the Ti-6Al-7Nb sample, uncoated and HA coated, in Hank's aerated solution at 37 °C, are shown in Figure 4. Both curves present approximately the same corrosion potential: −347 mV (SCE) for the uncoated sample and −323 mV (SCE) for the HA-coated sample. However, their shapes are considerably different.

From the corrosion potential to approximately 0 mV (SCE), the uncoated Ti-6Al-7Nb polarization curve has the typical behavior of activation polarization with an approximately linear variation, which suggests a probable compliance with the Tafel's law. The anodic Tafel slope (b_a) of this straight line is approximately 300 mV/decade. From 0 mV (SCE) to about 1200 mV (SCE) the curve displays an essentially passive behavior with a passive current density (i_{pp}) of about 10^{-6} A/cm^2. At about 1200 mV (SCE) the current density starts to increase, reaches a maximum of 8×10^{-6} A/cm^2 at about 1750 mV (SCE), and then decreases to about $5–6\times10^{-6}$ A/cm^2, suggesting transpassive behavior.

The polarization curve of the HA-coated alloy is quite anomalous. The potential range typical of activation polarization is very small. At approximately −250 mV (SCE) the curve already assumes passive behavior with a passive current density (i_{pp}) of about 2×10^{-7} A/cm^2. This passivity,

TABLE II. Semiquantitative Chemical Composition of Hydroxyapatite (HA) Coating Determined by EDS Analysis

	Element						
	Ca	P	Mg	Cl	Na	O	C
wt%	33.75	12.39	0.69	0.31	0.07	43.68	9.11

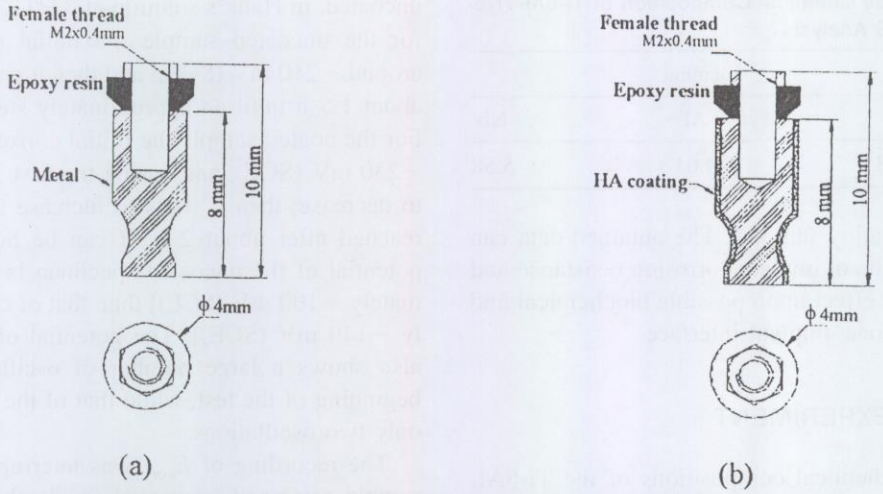

Figure 1. Shape of the (a) uncoated and (b) HA-coated cylindrical implants.

however, holds only for about 450 mV. At about 200 mV (SCE) the current density starts to increase, and this increase is roughly linear, reaching a value close to 8×10^{-4} A/cm^2 at approximately 1800 mV (SCE). For higher potentials the current density decreases slightly, and at 2500 mV (SCE) its value is about 6×10^{-4} A/cm^2.

Under deaerated conditions, the typical polarization curves obtained for both uncoated and HA coated alloys are shown in Figure 5. These curves are significantly different from those obtained in aerated solution. For better visualization they were plotted in Figures 6 and 7,together with the corresponding curves obtained in aerated solution. The first difference, which was expected, is the considerably lower corrosion potential displayed by both curves. For the uncoated alloy this potential dropped to −902 mV (SCE), while for the HA coated alloy it dropped to –538 mV(SCE).

As observed in Figure 6, the polarization curve of uncoated alloy obtained in the deaerated solution does not display the passive behavior in the range of 0–1200 mV(SCE) that is present in aerated solution. Above 1200 mV (SCE) the behavior is similar to that of aerated solution, but the current densities are about four times larger. Between the corrosion potential and 0 mV (SCE) the curve in deaerated solution presents two regions of approximately constant current density, the first at about 5×10^{-8} A/cm^2, and the second at about 2×10^{-7} A/cm^2.

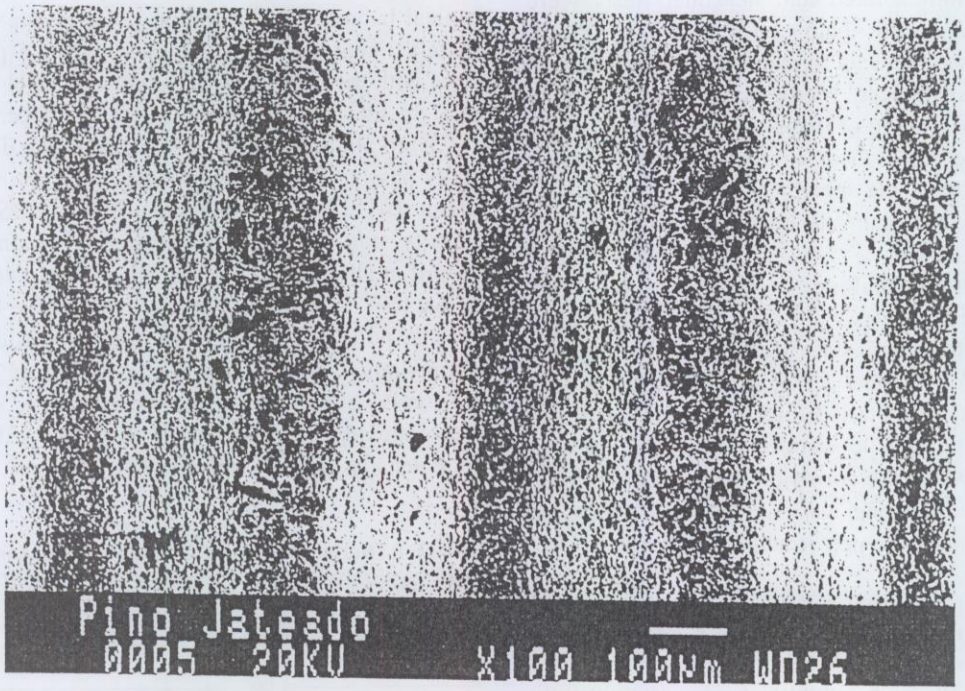

Figure 2. –Hydroxyapatite-coated surface of the implant screw. Note that the metallic surface is totally covered and that the coating is porous. SEM micrograph. 250×.

TABLE III. Chemical Composition of Hank's Solution

Component	Concentration (mol/l)
NaCl	0.1369
KCl	0.0054
$MgSO_4.7H_2O$	0.0008
$CaCl_2.2H_2O$	0.0013
$Na_2HPO_4.2H_2O$	0.0003
KH_2PO_4	0.0004
$C_6H_{12}O_6H_2O$	0.0050
Red phenol 1%	0.0071

The polarization curve of HA-coated alloy obtained in dearated solution has, as can be observed in Figure 7, a very similar shape to that obtained in aerated solution. The primary difference, besides that of corrosion potential, is the larger passive current density (i_{pp}) of about 4×10^{-7} A/cm^2.

The approximate corrosion current density (or corrosion rate) (i_{corr}) values were determined by extrapolating the cathodic part of polarization curves to the corrosion potential (E_{corr}). The average extrapolated values are presented in Table IV, together with the average values of E_{corr}. The obtained averages and the respective standard deviations (σ) refer to nine tests undertaken in aerated solution and three tests in deaerated solution. Note that the corrosion rates of uncoated samples are lower than those of HA-coated samples. Moreover, the deaeration of the Hank's solution resulted in a further decrease of these rates.

DISCUSSION

The corrosion potential variation with time curves, shown in Figure 3, are typical of passive metals immersed in aerated solutions. The corrosion potential of these metals is defined by the intersection of the passive anodic curve (which can be assumed as a straight line) with the cathodic curve of oxygen reduction reaction ($O_2 + 2H_2O + 4e \rightarrow OH^-$) in the range

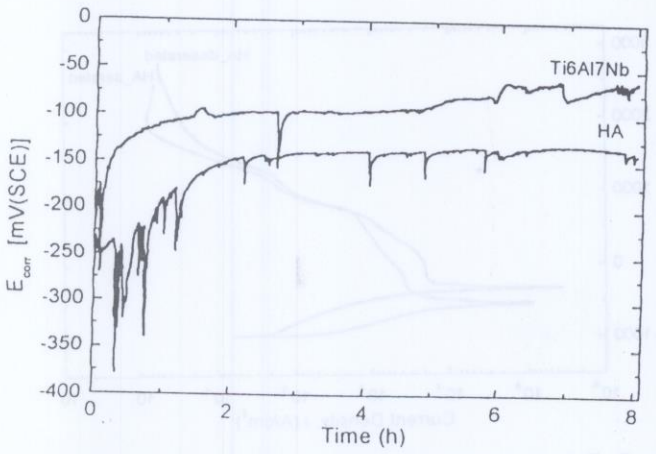

Figure 3. Corrosion potential, E_{corr}, variation with time of Ti-6Al-7Nb alloy uncoated and HA coated in Hank's solution at 37 °C.

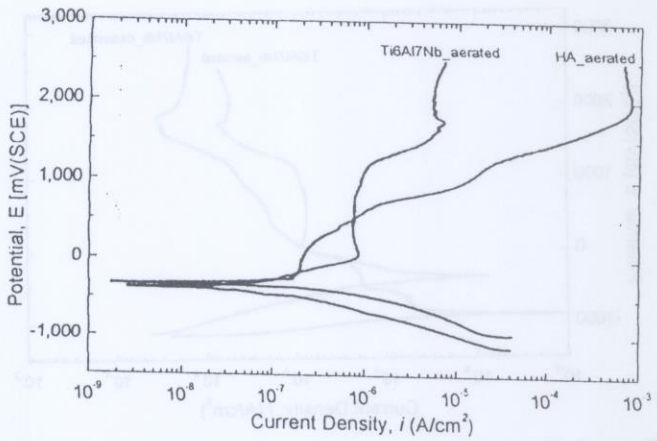

Figure 4. Potentiodynamic polarization curves of Ti-6Al-7Nb alloy uncoated and HA coated in Hank's aerated solution at 37 °C. Scanning rate: 1 mV/s.

where it displays activation polarization behavior. Just after the immersion, there is a transition stage during which the air-formed passive film may eventually undergo a partial dissolution that causes the potential to drop. However, as soon this stage is over, the passive film usually becomes more protective (possibly due to an increase in thickness), so that the passive current density (i_{pp}) tends to decrease. As a consequence, the intersection of the passive straight line with the cathodic curve is shifted to higher potentials. Thus, the corrosion potential increases until the passive film reaches its limiting protective capacity, resulting in stabilization of the corrosion potential.

For the uncoated sample the corrosion potential increases after its immersion, and it was found that this increase holds a logarithmic relationship with time for up to about 1.6 h. Similar behavior was observed by El-Basiouny and Mazhar,[12] who found that pure titanium (99.9%) in 0.5-N Na_2SO_4 solutions for times of more than 200 min also displays this type of relationship, which they ascribed as being due to the growth of passive oxide film.

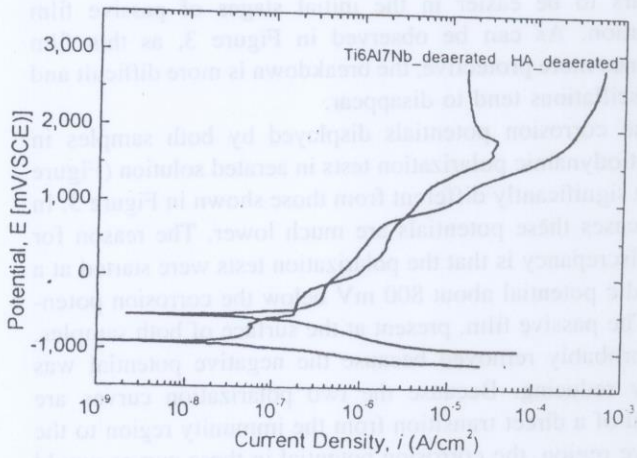

Figure 5. Potentiodynamic polarization curves of Ti-6Al-7Nb alloy uncoated and HA coated in Hank's deaerated solution at 37 °C. Scanning rate: 1 mV/s.

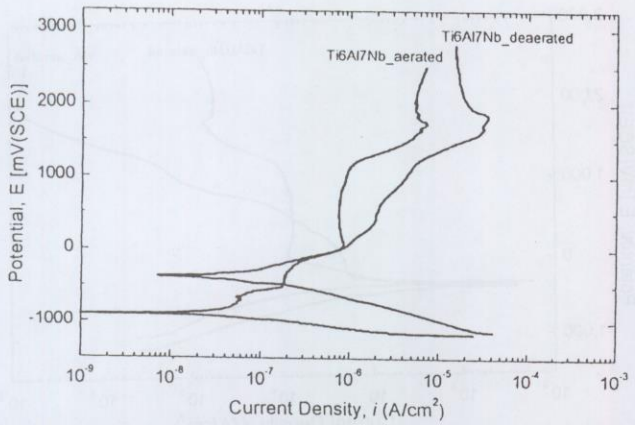

Figure 6. Potentiodynamic polarization curves of uncoated Ti-6Al-7Nb alloy in Hank's aerated and deaerated solutions at 37 °C. Scanning rate: 1 mV/s.

The lower corrosion potential exhibited for samples coated with hydroxyapatite appears to be associated with the porous character of this coating. It seems that the areas of the metallic alloy exposed to the pores determine this potential. The corrosion potential should be defined in a similar way as described above, but now the oxygen-reduction cathodic reaction would be more polarized, so that the intersection of both curves will take place at lower potentials. It is reasonable to expect that the oxygen content inside the pores is smaller than at the surface. Thus, the exchange current density of oxygen reduction reaction will also be smaller and, consequently, its cathodic reaction will become more polarized. It is also possible that the equilibrium potential of this reaction also becomes lower, mainly if there is a pH increase. This decrease will shift the cathodic curve as a whole to lower potentials so that the intersection with the passive straight line will also occur in lower potentials.

The oscillations observed on the corrosion potential variation with time curve for HA-coated samples suggests the occurrence of passive film breakdown, in a similar way as for pit nucleation and repassivation. The smaller oxygen availability inside the pores seems to favor this breakdown, and it appears to be easier in the initial stages of passive film formation. As can be observed in Figure 3, as this film becomes more protective, the breakdown is more difficult and the oscillations tend to disappear.

The corrosion potentials displayed by both samples in potentiodynamic polarization tests in aerated solution (Figure 4) are significantly different from those shown in Figure 3. In both cases these potentials are much lower. The reason for this discrepancy is that the polarization tests were started at a cathodic potential about 800 mV below the corrosion potential. The passive film, present at the surface of both samples, was probably removed because the negative potential was highly reducing. Because the two polarization curves are typical of a direct transition from the immunity region to the passive region, the corrosion potential in these curves would be defined by the intersection of the activation polarization anodic curve related to the formation of passive film (such as for example $Ti + 2H_2O \rightarrow TiO_2 + 4H^+ + 4e$) with the activation cathodic curve of oxygen reduction reaction. This intersection takes place in lower potentials than when there is already a well-formed passive film on the surface.

The further decrease in corrosion potential caused by the deaeration of the testing solution (see Figures 6 and 7) is expected since the cathodic reaction changes from oxygen reduction to hydrogen reduction ($H^+ + e \rightarrow H_2$), whose equilibrium potential is approximately 1.3 V lower.

The large difference observed in Figure 4 between the polarization curves obtained for the two samples in aerated solutions seems to be primarily associated with the availability of oxygen at the metallic surface. As was already pointed out, it is reasonable to expect that the oxygen content inside the pores of HA coating is less than at the surface. For the uncoated alloy, sufficient oxygen is available to maintain and/or repair the surface oxide, whereas for the HA-coated samples the available oxygen is insufficient. The tests carried out in deaerated solution support this hypothesis. As can be observed in Figure 5 under deaerated conditions the behavior of the anodic polarization curve of uncoated samples is very similar to that of the HA-coated samples up to approximately 1000 mV (SCE).

The transpassive behavior displayed by the uncoated alloy above 1200 mV (SCE) in aerated solution can be related to the oxidation[13] of TiO_2 to Ti_2O_5. However, as the solution contains other species, there is always the possibility of formation of other titanium compounds such as $NaTiOPO_4$.[14]

The constant dissolution rate through the passive film that is usually observed in the passive region is because any increase in the potential is accompanied by progressive thickening of the film, which maintains the electric field within it constant.[15] Thus, the presently observed continuous increase in current density with the increase of potential when the oxygen supply is limited or nonexistent seems to imply that the oxygen is essential for the growth of the passive film. A possible explanation is that the oxide film growth is accompanied by an acidification of the solution. This acidification is easily attained because the TiO_2 formation is accompanied, as

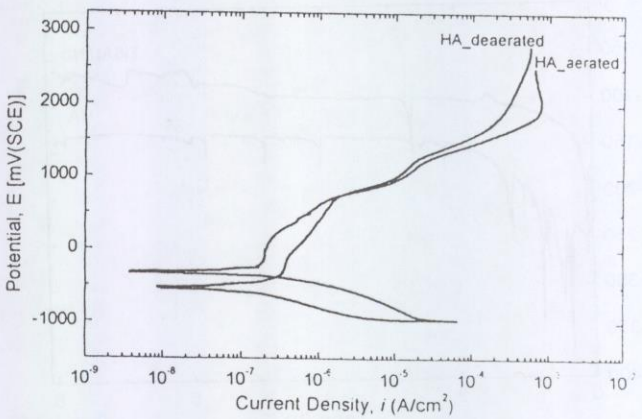

Figure 7. Potentiodynamic polarization curves of HA coated Ti-6Al-7Nb alloy in Hank's aerated and deaerated solutions at 37 °C. Scanning rate: 1 mV/s.

TABLE IV. Corrosion Potentials (E_{corr}) and Corrosion Current Densities (i_{corr}) of Uncoated and Coated with Hydroxyapatite (HA) Ti-6Al-7Nb Alloy in Hank's Aerated and Dearated Solution at 37 °C. Values Determined from Polarization Curves

Sample	Aerating conditions	$E_{corr} \pm \sigma$ mV (SCE)	$i_{corr} \pm \sigma$ $\mu A/cm^2$
Uncoated Ti-6Al-7Nb	Aerated	−347 ± 10 (9)	0.08 ± 0.03 (9)
	Deaerated	−902 ± 19 (3)	0.05 ± 0.01 (3)
HA-coated Ti-6Al-7Nb	Aerated	−323 ± 15 (9)	0.35 ± 0.14 (9)
	Deaerated	−538 ± 21 (3)	0.13 ± 0.05 (3)

The number of tests is indicated in parentheses.

shown above, by the formation of four hydrogen ions. The pH decrease could then be responsible for a faster dissolution of the oxide film. On the other hand, when the oxygen is present, the oxygen reduction reaction would be responsible for the release of OH^- ions, which would then neutralize the hydrogen ions produced during the TiO_2 film growth.

Cabrini et al.[8] proposed that the increase in the passive current density of HA-coated implant comparatively to uncoated may be ascribable to the presence of occluded corrosion cell formation under the pores present in the HA deposits. According to these authors the corrosion cell is established between the shielded portion (anode) and the unshielded surface (cathode). However, the polarization behavior of uncoated samples in deaerated solution indicates that the low oxygen content inside the HA-coating pore facilitates the acidification, making the electrolyte of this cell much more aggressive.

This pH decrease inside the pores of the HA coating can also explain the higher corrosion-rate values (i_{corr}) of HA-coated samples (see Table IV). As already pointed out, the TiO_2 formation is accompanied by the formation of four hydrogen ions. At the metal surface these ions are readily dispersed into the bulk solution, but inside the pores they tend to be retained, so that the pH decreases.

It must be stressed here that the above results were obtained for the initial conditions of immersion inside the Hank's solution. Long-term tests that are under way, however, indicate that after about 6 months of immersion in this solution, the electrochemical behavior of both samples experiences a significant change. The results of these tests will be published in due time.

CONCLUSIONS

1. The hydroxyapatite coating promotes a significant change in electrochemical behavior of Ti-6Al-7Nb alloy inside the Hank's solution.
2. The corrosion potential of both the coated and uncoated alloys tends to become stable with time, but for the coated sample the time for stabilization is longer (about 2 hours) than for the uncoated (about 1.5 hours). Moreover, the corrosion potential of an uncoated sample is always more noble than that of coated one.
3. The shape of potentiodynamic polarization curves is strongly affected by aerating conditions inside the testing solution. In aerated solutions the polarization curve of an uncoated sample shows typical passive/transpassive behavior, whereas in deaerated solutions this curve is similar to that of HA-coated sample, in which the current density continuously increases with the increase of the potential. Apparently this continuous increase in potential is controlled by acidification of the solution due to the TiO_2 oxide film formation, which is neutralized when there is a supply of elemental oxygen by the oxygen reduction reaction.
4. The corrosion rates of both coated and uncoated samples in either aerated or deaerated conditions, determined from polarization curves, are lower than 1 $\mu A/cm^2$, and are typical of passive behavior. However, the corrosion rate of coated samples is more than two times larger than that of uncoated ones. Even so, it is believed that at this level this corrosion will have negligible effect upon biochemical and cellular events at the bone–implant interface.

REFERENCES

1. Park E, Condrate Sr. R A, Hoelzer DT, Fischman GS. Interfacial characterization of plasma-spray coated calcium phosphate on Ti-6Al-4V. J Mater Sci Mater Med 1998;9:643–649.
2. Sergo V, Sbaizero O, Clarke DR. Mechanical and chemical consequences of the residual stresses in plasma sprayed hydroxyapatite coatings. Biomaterials 1997;18:477–482.
3. Lavos-Valereto IC, König Jr. B, Rossa Jr. C, Marcantonio Jr. E, Zavaglia AC. A study of histological responses from Ti-6Al-7Nb alloy dental implants with and without plasma-sprayed hydroxyapatite coating in dogs. J Mater Sci Mater Med 2001; 12:273–276.
4. Sridhar TM, Arumugam TK, Rajeswari S, Subbaiyan M. Electrochemical behaviour of hydroxyapatite-coated stainless steel implants. J Mater Sci Lett 1997;16:1964–1966.
5. Ducheyne P, Radin S, Heughebaert M, Heughebaert JC. Calcium phosphate ceramic coatings on porous titanium: Effect of structure and composition on electrophoretic deposition, vacuum sintering and in vitro dissolution. Biomaterials 1990;11: 244–254.
6. Lavos-Valereto IC. Characterization of Ti-6Al-7Nb alloy dental implants coated with hydroxyapatite by plasma-spray technique. Doctor thesis, IPEN—Institute for Energy and Nuclear Research, University of São Paulo (USP). São Paulo, Brazil; 1998. p. 129 (in Portuguese).
7. Sousa SR, Barbosa MA. The effect of hydroxyapatite thickness on metal ion release from Ti6Al4V substrates. Biomaterials 1996;17:397–404.
8. Cabrini M, Cigada A, Rondelli G, Vicentini B. Effect of different surface finishing and of hydroxyapatite coatings on pas-

sive and corrosion current of Ti6Al4V alloy in simulated physiological solution. Biomaterials 1997;18:783–787.
9. Leadley SR, Davies MC, Ribeiro CC, Barbosa MA, Paul AJ, Watts JF. Investigation of the dissolution of the bioceramic hydroxyapatite in the presence of titanium ions using ToF-SIMS and XPS. Biomaterials 1997;18:311–316.
10. González JEG, Mirza-Rosca JC. Study of the corrosion behavior of titanium and some of its alloys for biomedical and dental implant applications. J Electroanal Chem 1999;471:109–115.
11. Lavos-Valereto IC, Wolynec S, Deboni MCZ, König Jr. B. In vitro and in vivo biocompatibility testing of Ti-6Al-7Nb alloy with and without plasma-sprayed hydroxyapatite coating. J Biomed Mater Res 2001;58:727–733.
12. El-Basiouny MS, Mazhar AA. Electrochemical behavior of passive layers on titanium. Corrosion 1982;38:237–240.
13. Eliades T. Passive film growth on titanium alloys: Physicochemical and biologic considerations. Int J Oral Maxillofac Implants 1997;12:621–627.
14. Considine DM, editor. Van Nostrand's scientific encyclopedia (5th ed.). New York: Van Nostrand; 1976. pp 2210–2212.
15. West JM. Electrodeposition and corrosion processes (2nd ed.). London: Van Nostrand; 1970. p 87.